

## A WIRELESS POWER TRANSFER SYSTEM DESIGN FOR CHARGING OF INTRA-BODY IMPLANT DEVICES

*Edanur BÜYÜKTUNA* \*<sup>ID</sup>

*Elif DİLEK* \*<sup>ID</sup>

*Fatma Nur KARTAL* \*<sup>ID</sup>

*Ramazan ÇETİN* \*<sup>ID</sup>

*Ali AĞÇAL* \*<sup>ID</sup>

Received: 22.03.2023; revised: 16.11.2023; accepted: 09.01.2024

**Abstract:** Wireless power transfer (WPT) presents numerous possibilities for recharging electronic devices in challenging environments. Charging of biomedical devices within the body is among the available opportunities. Inductively coupled WPT is a dependable and effective solution for powering these devices. Energy is transferred from the transmitter to the receiver in the inductively coupled WPT system through the use of coils and magnetic coupling. A WPT system was designed for this study, with dimensions of 4 cm by 4 cm, power output of 1 mW, and a frequency of 13.56 MHz. Series-Series (SS) topology was selected for its ease of handling and simple architecture. A square coil was selected as the receiver and transmitter coil structure due to its higher coupling factor than circular coils. ANSYS® Maxwell 3D was used to design the coils and perform magnetic analysis. In the ANSYS® HFSS program, the WPT system was placed inside the male human model and the electromagnetic exposure of the WPT on humans was examined. The magnetic scattering of the WPT system was within the safe values specified by IEEE and ICNIRP standards.

**Keywords:** Wireless Power Transfer, Biomedical devices, Implant devices, Wireless charging

### Vücut İçi İmplant Cihazların Şarjı için Kablosuz Enerji Transfer Sistemi Tasarımı

**Öz:** Kablosuz enerji transferi (KET), zorlu ortamlarda elektronik cihazları şarj etmek için çok sayıda olanak sunar. Biyomedikal cihazların vücuttan şarj edilmesi de mevcut imkanlar arasındadır. Endüktif bağlantı ile birleştirilmiş kablosuz güç aktarımının kullanılması, bu cihazlara güç sağlamak için güvenilir ve etkili bir çözümdür. Endüktif olarak bağlanmış KET sisteminde vericiden alıcıya enerji, bobinler ve manyetik bağlantı kullanılarak aktarılır. Bu çalışma için 4 cm'ye 4 cm boyutlarında, 1 mW güç çıkışı ve 13,56 MHz frekansta bir WPT sistemi tasarlanmıştır. Seri-Seri (SS) topoloji, kullanım kolaylığı ve basit mimarisi nedeniyle seçilmiştir. Dairesel bobinlere kıyasla daha yüksek kuplaj faktörü nedeniyle alıcı ve verici bobin yapısı olarak kare bir bobin seçilmiştir. Bobinleri tasarlamak ve manyetik analizleri yapmak için ANSYS® Maxwell 3D kullanıldı. ANSYS® HFSS programında KET sistemi erkek insan modelinin içine yerleştirilmiş ve KET'in insanlar üzerindeki elektromanyetik maruziyeti incelenmiştir. KET sisteminin manyetik saçılımının IEEE ve ICNIRP standartlarında belirtilen güvenli değerler içerisinde olduğu görülmüştür.

**Anahtar Kelimeler:** Kablosuz Enerji Transferi, Biyomedikal cihazlar, İmplant cihazlar, Kablosuz şarj

\* Süleyman Demirel Üniversitesi, Mühendislik Fakültesi, Elektrik-Elektronik Mühendisliği Bölümü, 32200, Merkez/İsparta

It is an expanded version of the paper titled '1 mW Wireless Power Transfer System Design', which was presented orally at the ELECO'2022 Symposium and was invited by the symposium executive board to be evaluated in the Uludağ University Journal of the Faculty of Engineering.

Corresponding Author: Ali AĞÇAL (aliagcal@sdu.edu.tr)

## 1. INTRODUCTION

Electronic devices have become an integral part of our lives. Thanks to the advancements in technology, they are used in the field of human health and many other areas. The energy stored in the batteries of the internally implanted devices gets depleted over time. Changing these devices' batteries carries a great risk of infectious diseases for the patient and the risk of complications in the surgery. For this reason, the WPT system can eliminate many risks by charging these devices. Although WPT systems have lower efficiency than wired transmission, they are a much more reliable system (Karakaya, 2007). In cable transmissions, too much cable pollution occurs, and it also brings different problems that are not as innocent as cable pollution. The most important and vital risk of energy transmission by cable is for biomedical implants placed inside the body.

Active in-body implants (AIMD) are medical devices that work with electrical energy and are surgically implanted in the human body. Intrabody implants can analyse electrical mechanical signals. One of the biggest problems for AIMD is that it is not long-term. When the battery is discharged, it may require surgical intervention (Campi, et al., 2016). Since the battery replacement will be achieved through surgery, this condition can cause inflammation and various infections. These problems can be prevented with WPT. Wireless pacemaker charging is the most widely used intrabody implant charging (Demirci, 2020). It is an important problem that the pacemaker, which is used in diseases such as heart failure, that causes serious problems that can end human life, is replaced when the charge is exhausted.

A pacemaker is used in diseases such as heart failure and rhythm disorders, which are among cardiovascular diseases and result in death if not treated. Pacemakers are divided into temporary pacemakers and permanent pacemakers. Temporary pacemakers are used temporarily to regulate the heart rhythm of a person with rhythm disorders or until a permanent pacemaker is inserted. They are larger than permanent pacemakers and can cause various vascular diseases. As for, permanent pacemakers have a lower risk. A pacemaker is placed by creating a pocket under the skin on the left upper chest. The most widely used pacemakers are lithium-ion batteries (Demirci, 2020). Although lithium-ion batteries are known to last a long time, they still do not have infinite power and have a lifespan of 5-10 years. Charging with WPT is much more advantageous, considering the negative effects of the processes required to replace the battery.

WPT has been provided by microwave (Brown, 1969), electromagnetic radiation (Tesla, 1905), laser (Sahai and Graham, 2001), energy harvesting (Shuvo, et al., 2022), capacitive coupling (Dai and Ludois, 2015) and inductive coupling methods (Sample, et al., 2015). Among these methods, inductive coupling is the most used and most suitable method for charging implant devices (RamRakhyani, et al., 2010). One of the application areas of inductively coupled WPT is recharging implanted devices in biomedicine (Agarwal, et al., 2017). The WPT is used in many application areas such as pacemaker (Campi, et al., 2016), cochlear implant (Hong, et al., 2020), and peripheral nerve implant (Jegadeesan, et al., 2015) charging. Dimensions, powers and operating frequencies vary according to application areas (Agarwal, et al., 2017).

In this paper, energy was transferred from a transmitter to a receiver through magnetic coupling via coils. The present study designed a WPT system with an outer diameter of 4 cm by 4 cm, a power output of 1 mW, and a frequency of 13.56 MHz. The receiver and transmitter coils were designed in a square shape, offering a higher coupling factor than circular structures. Ansys Maxwell 3D simulation program and square coil inductance equations were used in the coil design. The exposure of the WPT system on human health was also investigated using the ANSYS® HFSS program and was compared with IEEE and ICNIRP standards. The study found that the magnetic scattering of the WPT system was below the exposure limit values specified by IEEE and ICNIRP standards, indicating that the system is safe for human use.

## 2. WPT SYSTEM WITH INDUCTIVELY COUPLING

Inductively coupled WPT uses magnetic coupling to transfer electrical energy between two systems. This technology is used to charge a variety of applications where there is reliability, freedom of movement, and no cable pollution is desired. The main purpose of WPT is to efficiently transfer the energy stored in the transmitter coil to the secondary coil. The inductive coupled WPT system uses from the resonance structure to transfer energy efficiently. In order to compensate the inductive reactive power of the coils, capacitors are added in series or parallel to the transmitter and receiver coils. Both the transmitter and receiver become resonant circuits and are tuned to the same resonant frequency to increase the efficiency of power transmission. This type of inductive power transfer is known as magnetic resonance coupling (Imura and Hori, 2011). If there are inductors and capacitors in electrical circuits, oscillations occur between these elements at certain frequencies. The frequency with the highest oscillation is called the resonance frequency. A simple resonator circuit consisting of a capacitor, inductor and resistor is shown in Figure 1.

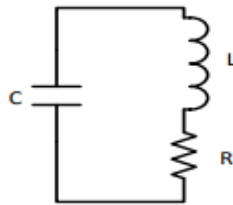


**Figure 1:**  
*Resonator Circuit*

where,  $L$  is the coil,  $C$  is the capacitor and  $R$  is the internal resistance. Energy oscillates between the coil and capacitor at the resonant frequency and is dissipated in the resistor. The term quality factor ( $Q$ ) is used to indicate the efficiency of this circuit and this term was shown by (1). It has no unit. The natural resonant frequency  $\omega_0$  of the resonator has been denoted by (2).

$$Q = \sqrt{\frac{L}{C} \frac{1}{R}} = \frac{\omega_0 L}{R} \quad (1)$$

$$\omega_0 = \frac{1}{\sqrt{LC}} \quad (2)$$

Different topologies are used in magnetic resonance coupling circuits. These topologies are named according to the way the capacitor in the circuit is connected to the coils. The main compensation topologies are serial-serial (SS), serial-parallel (SP), parallel-serial (PS), parallel-parallel (PP). In addition to these 4 basic topologies, there are other topology structures derived from these topologies. In this study, SS topology was investigated due to its ease of control and high efficiency. In SS topology, capacitors are connected in series with the coils. The WPT system with SS topology is shown in Figure 2.

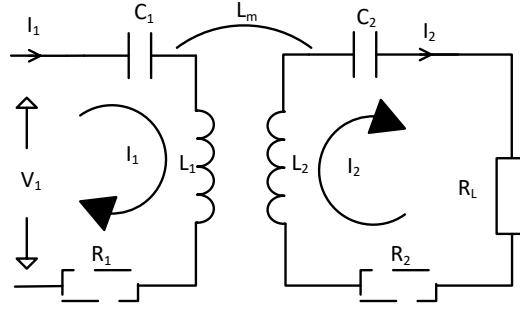


**Figure 2:**  
The WPT circuit with SS topology

where,  $V_1$  is the input voltage.  $I_1$  and  $I_2$  is input and output current, respectively.  $L_m$  is the mutual inductance.  $L_1$  and  $L_2$  represents inductance of the transmitter and the receiver coil, respectively.  $C_1$  and  $C_2$  is the capacitance of the transmitter and the receiver, respectively.  $R_L$  is the load resistance.  $R_1$  and  $R_2$  is internal resistance of the transmitter and the receiver, respectively. For simpler expression in formulas,  $Z_1=R_1+j\omega L_1$  and  $Z_2=R_2+j\omega L_2$  are expressed. The connection of two magnetically coupled coils is defined in (3) by the mutual inductance equation.

$$L_m=k\sqrt{L_1L_2} \quad (3)$$

Here  $k$  is the coupling factor and always takes a value between 0 and 1. The coupling coefficient is one of the basic parameters used in the efficiency calculation. In the WPT system, besides  $k$ , the quality factor is an important parameter for efficiency. Figure of merit ( $U$ ) is a result of  $k$  and the quality coefficient. Figure of merit is given in (4).

$$U = k\sqrt{Q_1Q_2} = \frac{\omega_0 L_m}{\sqrt{R_1R_2}} \quad (4)$$

$Q_1$  and  $Q_2$  are primary and secondary quality factors, respectively. Optimum efficiency is calculated using the Figure of merit. The optimum efficiency equation is given in (5).

$$\eta_{opt} = \frac{U^2}{(1+\sqrt{1+U^2})^2} \quad (5)$$

One of the most important parameters in the WPT system is the equivalent impedance and is denoted by  $Z_{Eq}$ . The equivalent impedance equation for the SS topology is given in (6) and the efficiency equation is given in (7) (Ağcal, et al., 2022).

$$Z_{Eq} = Z_1 + \left( \frac{1}{j\omega C_1} \right) + \left( \frac{L_m^2 \omega^2}{Z_2 + \frac{1}{j\omega C_2} + R_L} \right) \quad (6)$$

$$\eta = \left| \left( \frac{j\omega L_m}{Z_2 + \left( \frac{1}{j\omega C_2} \right) + R_L} \right)^2 \times \frac{R_L}{Z_{Eq}} \right| \quad (7)$$

In order to obtain maximum efficiency from the WPT system, the mutual inductance value must be greater than the critical mutual inductance ( $L_{merit}$ ). The critical mutual inductance calculation for the SS topology is given in (8) (Imura and Hori, 2011).

$$L^2_{m_{critical}} = \frac{R_L^2 - R^2}{\omega_0^2} \quad (8)$$

The fact that the mutual inductance is smaller than the critical mutual inductance causes the efficiency of the system to decrease. In this case, the system efficiency is below the maximum value and has a single resonance frequency. Maximum efficiency is achieved if the mutual inductance is above the critical mutual inductance value. In this case, bifurcation occurs in the resonant frequency. As the mutual inductance increases above the critical mutual inductance value, the frequency range between bifurcated frequencies increases.

### 3. COIL DESIGN

In order to obtain a high efficiency in the WPT system, it is necessary to determine the circuit parameters. The frequency of this study was determined as 13.56 MHz. Capacitance values for the receiver and transmitter in the circuit were calculated as  $C_1 = C_2 = 234.74$  pF and inductance values were calculated as  $L_1 = L_2 = 586.86$  nH. The load was chosen as  $5 \Omega$ . Critical mutual inductance value was calculated as  $L_{m_{critical}} = 58.67$  nH.

Planar square coil is used as coil design in WPT system. Planar spiral is preferred because the mutual inductance of planar spiral coils is higher than helical coils. In planar spiral coils, the square coil is preferred because the mutual inductance of the square coil is higher than that of the circular coil. Outside diameter ( $d_{out}$ ), inner diameter ( $d_{in}$ ), number of turns ( $N$ ), wire diameter ( $w$ ), and distance between wires ( $s$ ) parameters must be determined in a planar square coil. Different methods are used for the self-inductance of the planar square coil. The most commonly used self inductance calculation method is the Expression Based on Current Plate Approximation method. Self inductance equation of this method is given by (9) (Mohan, et al., 1999).

$$L = \frac{1.27\mu_0 N^2 d_{avg}}{2} \left( \ln \left( \frac{2.07}{\rho} \right) + 0.18\rho + 0.13\rho^2 \right) \quad (9)$$

Here,  $\mu_0$  is known as magnetic permeability and its value is  $4\pi \times 10^{-7}$  H/m.  $d_{avg}$  is the mean diameter (10) and  $\rho$  is the fill rate, it can be calculated with (11).

$$d_{avg} = \frac{d_{out} + d_{in}}{2} \quad (10)$$

$$\rho = \frac{d_{out} - d_{in}}{d_{out} + d_{in}} \quad (11)$$

$$d_{in} = d_{out} - 2N(w + s) + 2s \quad (12)$$

The coil parameters obtained for the determined inductance value are given in Table 1.

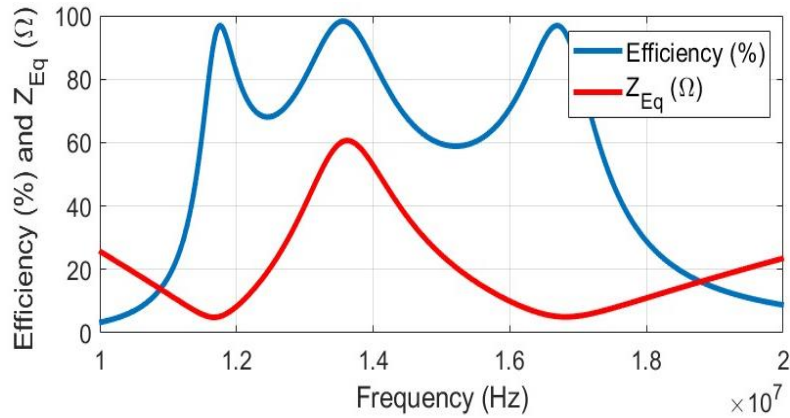
**Table 1. Coil parameters**

N	5
$d_{out}$	40 mm
$d_{in}$	6.7 mm
w	3.25 mm
s	0.1 mm
Wire length	528.65 mm
$R_{in}$	0.08 $\Omega$

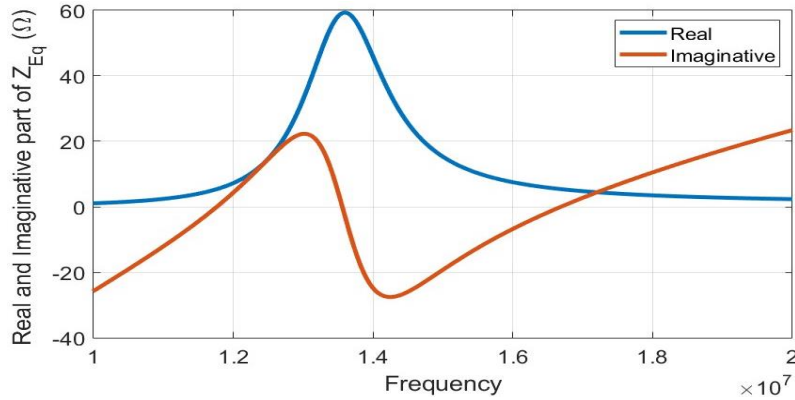
#### 4. SIMULATION STUDIES

##### 4.1. MATLAB/Simulink

The WPT system was investigated for low and high coupling factors. It was chosen as 0.35 for the case with a high coupling factor and 0.05 for the case with a low coupling factor. Using the efficiency (6) and equivalent impedance (7) equations given in Section 2, the change of equivalent impedance and efficiency according to frequency is investigated. In the SS topology, the graph of the change of equivalent impedance and efficiency according to frequency for the coupling factor value of 0.35 is given in Figure 3.



a.



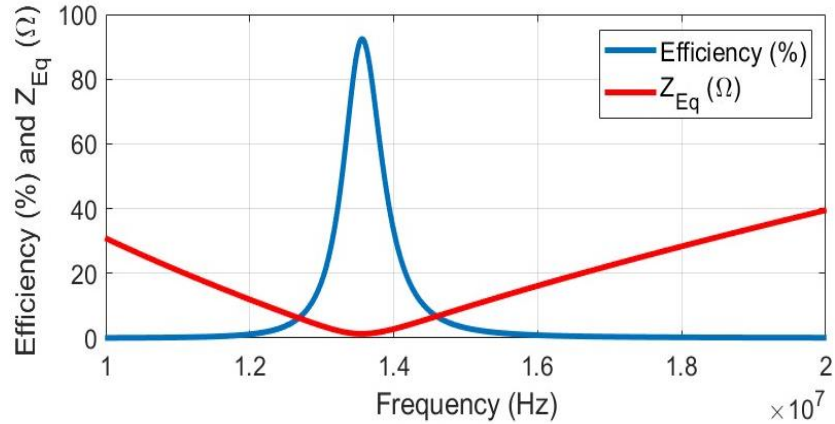
b.

**Figure 3:**

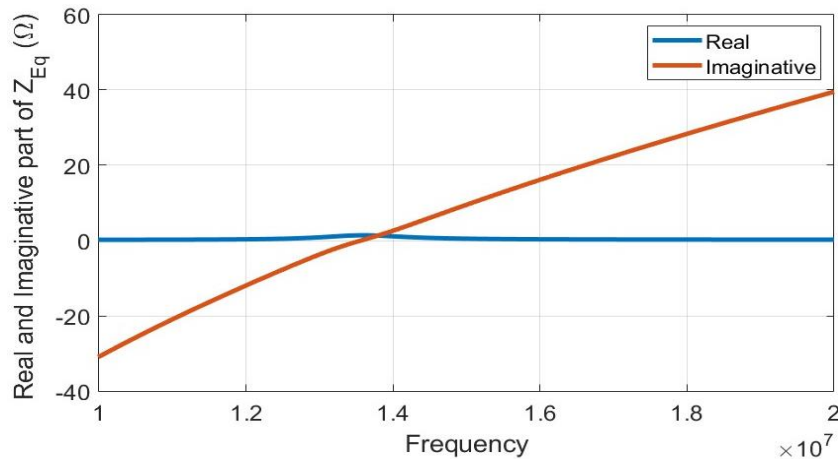
a. Efficiency and absolute  $Z_{Eq}$  and b. real and imaginative part of  $Z_{Eq}$  plot according to frequency for  $k=0.35$

For  $k=0.35$ , it can be seen from Figure 3 that there are bifurcations in the resonant frequency because the mutual inductance is above the critical value. There have been 3 separate resonances and using the second of these resonance frequencies is generally not a preferred method. Because the equivalent impedance is high in the second resonance frequency. This reduces the input power under the same voltage. Therefore, the second resonant frequency is not a desired operating region. When looking at the first and third resonant frequency points, it is seen that the system has the highest efficiency and the equivalent impedance is the lowest at these points. It can also be observed in Figure 3 that the efficiency is equal to 96.9% for the first and third resonance

frequencies. In applications, the first resonance frequency with a lower frequency is chosen because the skin effect and proximity effect losses are lower. The SS topology is also investigated for low coupling factor. The efficiency-frequency and equivalent impedance-frequency graphs for the coupling factor 0.05 are given in Figure 4.



a.



b.

**Figure 4:**

a. Efficiency and absolute  $Z_{Eq}$  and b. real and imaginative part of  $Z_{Eq}$  plot according to frequency for  $k=0.05$

Figure 4 shows that the resonant frequency is 13.56 MHz. Compensation of the WPT is fully achieved at resonance frequencies where the imaginary value of the equivalent impedance is zero. In Fig. 3 (b), the imaginary value of the equivalent impedance is zero at 3 separate frequencies. In Fig. 3 (a), the efficiency is maximum and the equivalent impedance is minimum at 3 different frequencies. In Fig. 4 (b), the imaginary value of the equivalent impedance is zero at 1 frequency. In Fig. 4 (a), there is only 1 resonance frequency. At this resonance frequency, the efficiency is maximum and the equivalent impedance is minimum. When Figure 3 and Figure 4 are compared, efficiency is high above the critical coupling factor and it is low below the critical coupling factor. If the coupling factor is below the critical coupling factor, the efficiency drops below the maximum value and as the coupling decreases, the efficiency decreases. When the coupling factor exceeds the critical coupling factor, the efficiency is maximum but the resonance frequency is bifurcated. The WPT circuit with SS topology in Figure 2 is set up in MATLAB/Simulink. Operating frequencies were determined from Figure 3 and Figure 4. MATLAB/Simulink results were given in Table 2.

**Table 1. MATLAB/Simulink parameters**

k = 0.35		k = 0.05	
Air gap = 15 mm	$L_m = 205.4 \text{ nH}$	Air gap = 24 mm	$L_m = 29.343 \text{ nH}$
$f = 11.76 \text{ MHz}$	$\eta_L = 96.9 \%$	$f = 13.56 \text{ MHz}$	$\eta_L = 92.42 \%$
$V_1 = 74.95 \text{ mV}$	$V_L = 72.58 \text{ mV}$	$V_1 = 38.18 \text{ mV}$	$V_L = 71.7 \text{ mV}$
$I_1 = 14.51 \text{ mA}$	$I_2 = 14.52 \text{ mA}$	$I_1 = 29.14 \text{ mA}$	$I_2 = 14.34 \text{ mA}$
$P_1 = 1.09 \text{ mW}$	$P_2 = 1.05 \text{ mW}$	$P_1 = 1.11 \text{ mW}$	$P_2 = 1.03 \text{ mW}$
$V_{c1} = 836.3 \text{ mV}$	$V_{c2} = 836.8 \text{ mV}$	$V_{c1} = 1457 \text{ mV}$	$V_{c2} = 717 \text{ mV}$

### 4.2 Maxwell 3D

According to the values obtained in Table 1, the coil was designed in the ANSYS® Maxwell 3D program. The designs were compared by adding core and shielding to the coil. A flexible ferrite sheet (Mull6060) with a thickness of 0.09 mm and size of 60 mm x 60 mm was used as the core. The relative magnetic permeability of this material for 13.56 Mhz is 150 (Laird, 2023). Aluminum material with a thickness of 0.1 mm and dimensions of 60 mm x 60 mm was used for shielding. The designed coil is shown in Figure 5.

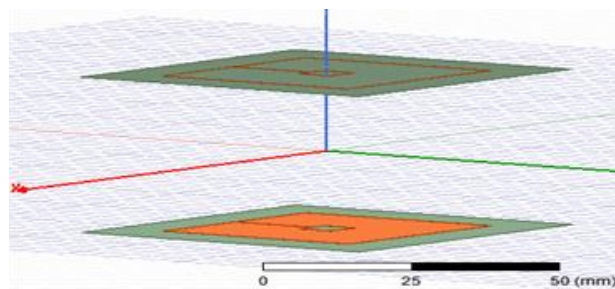


**Figure 5:**  
*Coil design in Maxwell 3D*

The mutual inductance values according to the air gap are shown in Figure 6. These values were analyzed in four different ways as unshielded-coreless, unshielded-cored, shielded-coreless, and shielded-cored.

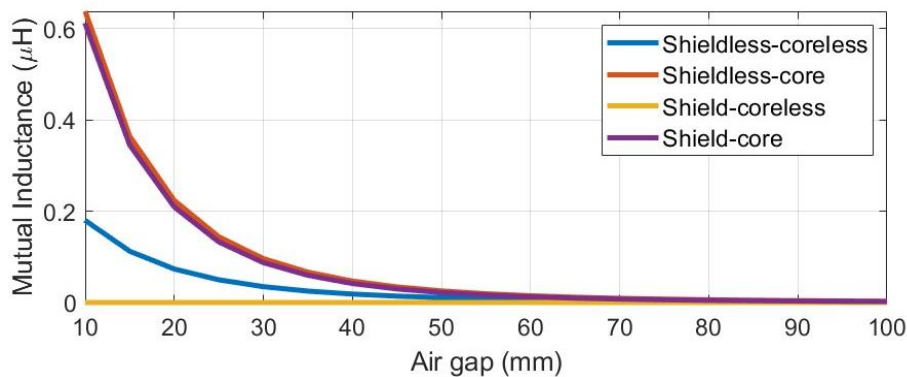


**Figure 6:**  
*Mutual inductance values according to the air gap*

When the graph is examined, it is seen that the lowest mutual inductance value is obtained in the shielded-coreless condition. The highest mutual inductance value was obtained in the case of only the core and shieldless. The change of the coupling factor according to different air gaps is shown in Figure 7. These values were also evaluated in terms of shielding and core.

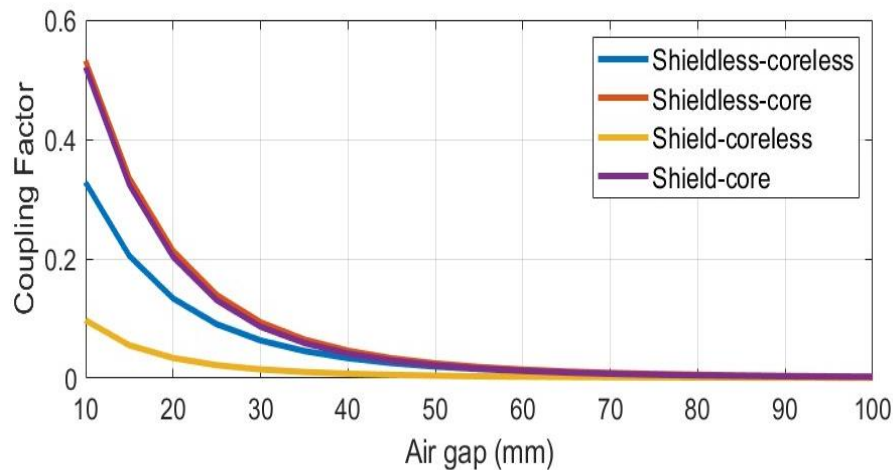


**Figure 7:**  
*Coupling factor according to the air gap*

In Figure 7, it is seen that the highest coupling factor is obtained in the lowest air gap and in the unshielded-core condition. It should not be overlooked that the coupling factor decreases significantly as the air gap increases. The worst coupling factor occurred in the shielded-coreless condition. When Figure 6 and Figure 7 are examined together, it is seen that the results are consistent. It is understood that there is too much loss if shielding is done without using a core. The coreless-shielded condition is not useful for design.

The highest mutual inductance and coupling factors are obtained in the unshielded-core condition. However, shielding is necessary to protect the implant device from magnetic interference. Core and shielded design is preferred, as shielding causes a tolerable link reduction when used with the core.

A shielding material is often used in wireless power transmission systems to minimize electromagnetic interference. The core is generally a ferromagnetic material such as ferrite. The core is used to help concentrate and direct the magnetic field created by the current passing through the conductors. The core increases the magnetic coupling, making wireless power transfer more efficient. It doesn't have the same effect when you place a shielding without a core because it doesn't affect the magnetic field similarly. The shield can only protect against electromagnetic interference, but it is not as effective as the core in focusing and directing the magnetic field. Essentially, the core improves the magnetic coupling between the transmitting and receiving coils, improving the overall performance of the wireless power transfer system. While the shield is still useful, it does not play a role in increasing magnetic coupling, it just protects from magnetic interference.

## 5. EFFECTS ON HUMAN HEALTH

Since the WPT is provided with a magnetic connection, magnetic and electrical field occurs between and around the receiver and transmitter coil. The electromagnetic exposure of the WPT system to be placed inside the body should be below the limit values according to the IEEE standard and ICNIRP guidelines. The exposure limit values for the 13.56 MHz WPT system are given in Table 3 (ICNIRP, 2010; IEEE,2019).

**Table 3. The electromagnetic exposure limit according to ICNIRP and IEEE standards (ICNIRP, 2010; IEEE,2019).**

Standards	Electric field		Magnetic field		Magnetic flux density	
	PUE	PRE	PUE	PRE	PUE	PRE
<b>IEEE (Head and chest)</b>	1842 V/m	614 V/m	163 A/m	490 A/m	205 $\mu$ T	615 $\mu$ T
<b>ICNIRP</b>	OE	PE	OE	PE	OE	PE
	170 V/m	83 V/m	80 A/m	21 A/m	100 $\mu$ T	27 $\mu$ T

PUE and PRE are the exposure limits in unrestricted environments and restricted environments, respectively. OE is an occupational exposure limit and PE is a public exposure limit. Simulations were carried out on the ANSYS® HFSS interface to analyze the effects of the coil design on humans. The male body was used in the simulation. The coil was designed for two different situations, with core and without core.

The receiving coil was placed approximately 1 cm inside the model's chest. As a result of this simulation, electric field (E field), magnetic field (H field), and specific absorption rate (SAR) images were obtained. The electric field acting on the human body is shown in Figure 8.

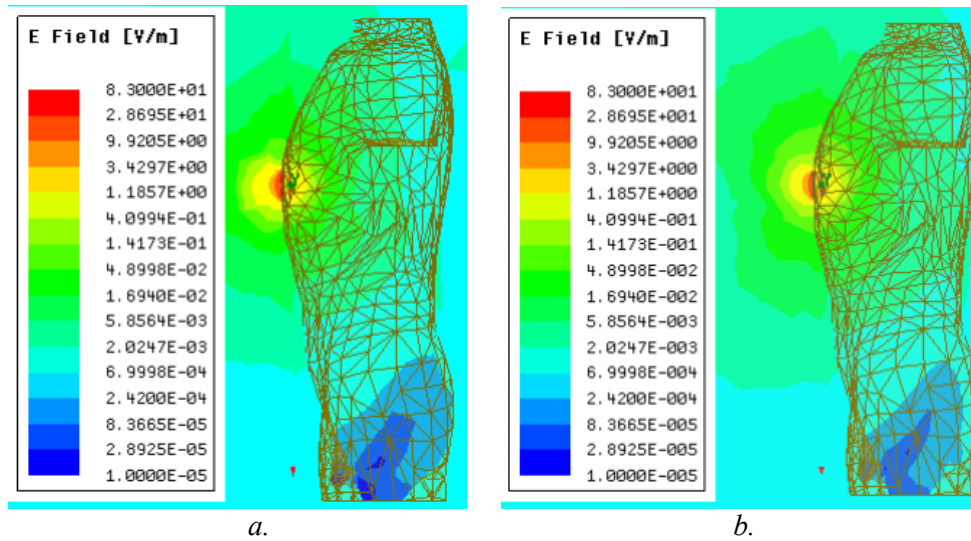


**Figure 8:**  
*Electric field in a. with core and b. coreless system*

The magnetic field affecting the human body is presented in Figure 9.

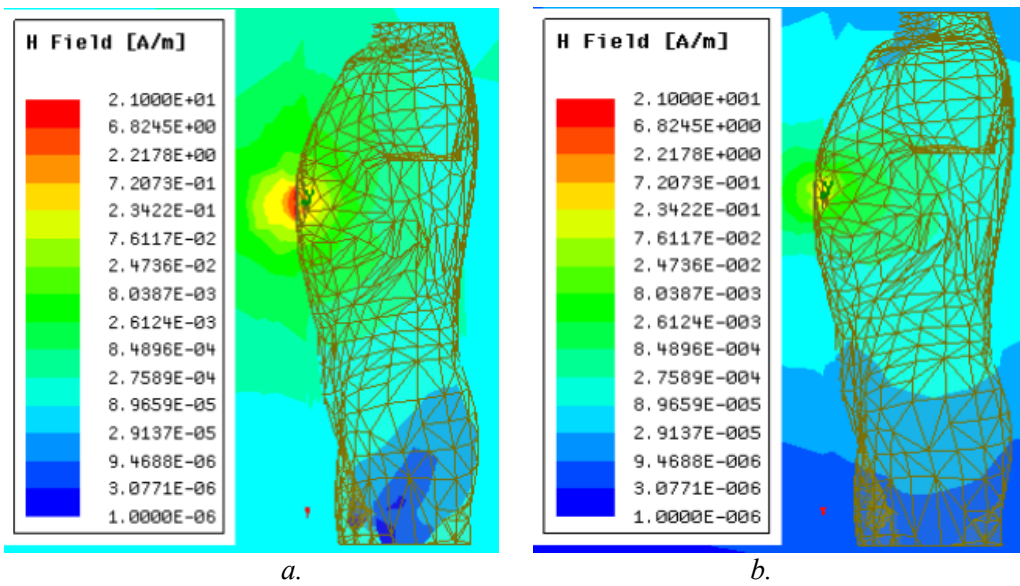


**Figure 9:**  
The magnetic field in a. with core and b. coreless system

The electric field, magnetic field and magnetic flux density of WPT designs from the midpoint of the receiver and transmitter to the inside of the chest are shown in Figure 10.

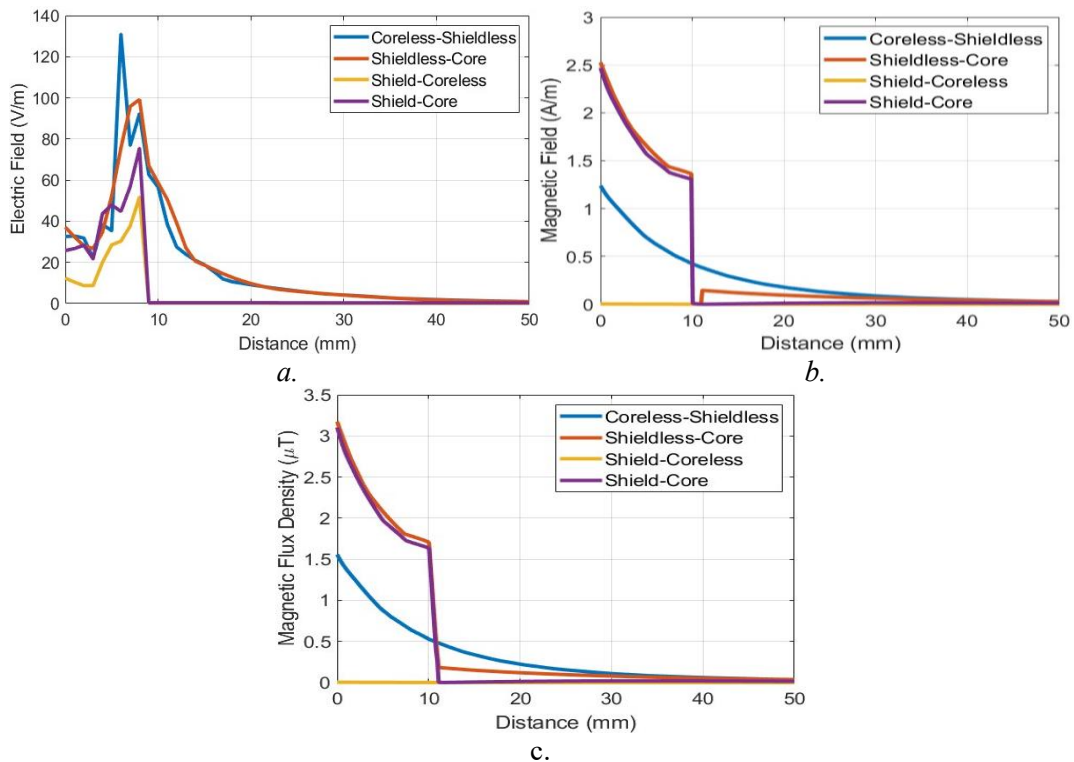


**Figure 10:**  
Electromagnetic field distributions of WPT designs: (a) Electric field, (b) magnetic field, and (c) magnetic flux density

Maximum electromagnetic exposure values created by WPT designs on the human chest are given in Table 4.

**Table 4. Maximum electromagnetic exposure values created by WPT designs on the human chest**

	Electric Field	Magnetic Field	Magnetic Flux density
Shieldless-Coreless	130.97 V/m	1.24 A/m	1.56 $\mu$ T
Shieldless-Core	99.22 V/m	2.53 A/m	3.17 $\mu$ T
Shield-Coreless	51.72 V/m	0.004 A/m	0.005 $\mu$ T
Shield-Core	75.42 V/m	2.47 A/m	3.10 $\mu$ T

When Table 4 and Figure 10 are examined, all designs' magnetic field and magnetic flux density values are below IEEE and ICNIRP standards. However, Shieldless-Coreless and Shieldless-Core designs are above ICNIRP public exposure limits for electric fields. Although the shield-coreless design seems suitable for the electric field, it is not preferred because it seriously weakens the magnetic coupling. As a result, the shield and core design is the most suitable design for human health. Additionally, this design complies with electromagnetic field exposure standards according to IEEE and ICNIRP.

SAR is a measure of the rate of energy absorbed by the body when exposed to an electromagnetic field. It is defined as the power absorbed per unit mass of tissue. As this value increases, the amount of radiation emitted by the electromagnetic source increases. The rate of absorption of electromagnetic energy by body tissues is shown in Figure 11.

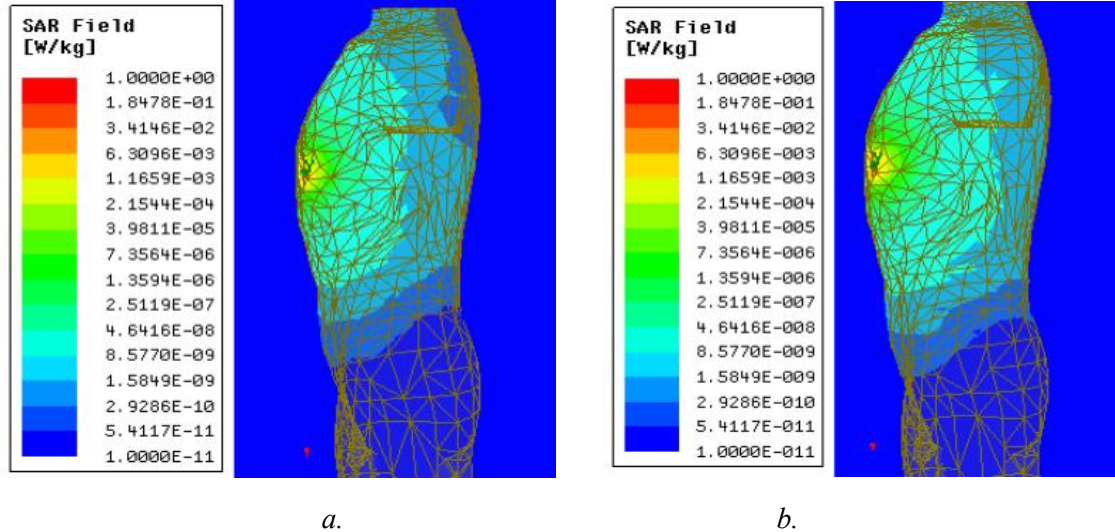


**Figure 11:**  
*SAR for a. with core and b. coreless system*

Although the heat effect differs according to the tissues, 4W/kg is the threshold value even for the most sensitive tissues. When the WPT system with core and coreless system are compared, both systems appear to have a SAR value of less than 4W/kg. In contrast, using the core and shield design, the human body is less affected by the electric field, magnetic field, and specific absorption rate. According to IEEE and ICNIRP standards, this design is below the exposure limit values for human health.

## 6. RESULTS

Wireless transmission of energy is an indispensable tool in the charging of intra-body implants since the transfer of energy by cable carries various infection risks. In this study, wireless energy transmission to a biomedical implant device was aimed. A pacemaker model was taken as a biomedical device. The WPT system was designed using the inductively coupling method. Circuits with SS topology are built in MATLAB/Simulink. The WPT system was investigated for the performance of four different coils with a 4 cm diameter, which included unshielded-core, unshielded-core, shielded-coreless, and shielded-core designs. The highest values of mutual inductance and coupling factor were observed exclusively in the configuration that included a core, and then in the configuration that included both a core and a shield.

Since AIMD devices directly affect human health, these devices have shielding material to protect them from magnetic interference. Since the pacemaker used has shielded itself, no extra shielding was needed in the coil design, and the current shielding is the device's own shielding. The effects of the system on human health were evaluated using the ANSYS® HFSS program with reference to IEEE and ICNIRP standards. When the WPT system was examined, it was observed that the SAR value affecting the human body is below 4W/kg in all 4 coil designs. Additionally, the human body was affected much less electromagnetic fields using coils with the core-shield. For this reason and because it increases the coupling factor, a cored-shielded system should be preferred in the design.

## ACKNOWLEDGMENTS

We thank Laird Company for sharing the Mull 6060 samples with us.

## CONFLICT OF INTEREST

Authors approve that to the best of their knowledge, there is not any conflict of interest or common interest with an institution/organization or a person that may affect the review process of the paper.

## AUTHOR CONTRIBUTION

Edanur BÜYÜKTUNA: Determination and management of the design, simulation processes of the study, and full responsibility

Elif DİLEK: Determination and management of the design, simulation processes of the study, and full responsibility

Fatma Nur KARTAL: Drafting the article, critical review of the content, and full responsibility

Ramazan ÇETİN: Creation of theoretical content and equations, management of the simulation process, drafting of the article, and full responsibility

Ali AĞÇAL: Methodology, reviewing, editing, and full responsibility.

## REFERENCES

1. Agarwal, K., Jegadeesan, R., Guo, Y. X., and Thakor, N. V. (2017) Wireless power transfer strategies for implantable bioelectronics, *IEEE reviews in biomedical engineering*, 10, 136-161. doi: 10.1109/RBME.2017.2683520

2. Ağçal, A., Doğan, T. H., and Aksu, G. (2022) The Effects of Operating Frequency on Wireless Power Transfer System Design and Human Health in Electric Vehicles, *Electrica*, 22(2), 188-197. doi: 10.54614/electrica.2022.22020
3. Brown, W.C. (1969) Experiments involving a microwave beam to power and position a helicopter, *IEEE Transactions on Aerospace and Electronic Systems*, 5(1), 692-702. doi: 10.1109/TAES.1969.309867
4. Campi, T., Cruciani, S., Palandrani, E., De Santis, V., Hirata, A., and Feliziani, M. (2016) Wireless Power Transfer Charging System for AIMDs and Pacemakers, *IEEE Transactions on Microwave Theory and Techniques*, 64(2), 633-642. doi: 10.1109/TMTT.2015.2511011
5. Dai, J., and Ludois, D. C. (2015) A survey of wireless power transfer and a critical comparison of inductive and capacitive coupling for small gap applications, *IEEE Transactions on Power Electronics*, 30(11), 6017-6029. doi: 10.1109/TPEL.2015.2415253
6. Demirci, Y.E. (2020). Kalp Pili Uygulamaları için kablosuz enerji transferi devre tasarımı, Master thesis, Pamukkale Üniversitesi, Türkiye.
7. Hong, S., Jeong, S., Lee, S., Sim, B., Kim, H., and Kim, J., (2020) Low EMF design of cochlear implant wireless power transfer system using a shielding coil”, *In 2020 IEEE International Symposium on Electromagnetic Compatibility & Signal/Power Integrity (EMCSI)*, Reno, 623-625. doi: 10.1109/EMCSI38923.2020.9191460
8. IEEE, (2019) Standard for safety levels with respect to human exposure to electric, magnetic, and electromagnetic fields (0 Hz to 100 kHz), Std, Vol. C95, no. 1<sup>TM</sup>-2019,.
9. Imura, T., and Hori, Y. (2011) Maximizing air gap and efficiency of magnetic resonant coupling for wireless power transfer using equivalent circuit and Neumann formula, *IEEE Transactions on industrial electronics*, 58(10), 4746-4752. doi: 10.1109/TIE.2011.2112317
10. International Commission on Non-Ionizing Radiation Protection (ICNIRP), (2010) Guidelines for limiting exposure to time-varying electric and magnetic fields for low frequencies (1 Hz–100 kHz),” *Health Physics*, 99(6), 818–836. doi: 10.1097/HP.0b013e3181f06c86
11. Jegadeesan, R., Nag, S., Agarwal, K., Thakor, N., and Guo, Y.-X. (2015) Enabling wireless powering and telemetry for peripheral nerve implants, *IEEE J. Biomed. Health Informat.*, 19(3), 958–970. doi: 10.1109/JBHI.2015.2424985
12. Karakaya, U., (2007) Motor control via wireless energy and information transfer”, Master thesis, İstanbul Teknik Üniversitesi, Türkiye.
13. Laird, (2023). Flexible Magnetic Sheet MULL6060-300. Erişim Adresi: <http://https://www.laird.com/products/inductive-components-emc-components-and-ferrite-cores/ferrite-sheets/mull-series/mull6060-300> (Erişim Tarihi: 09.11.2023)
14. Mohan, S. S., del Mar Hershenson, M., Boyd, S. P., and Lee, T. H. (1999) Simple accurate expressions for planar spiral inductances, *IEEE Journal of solid-state circuits*, 34(10), 1419-1424. doi: 10.1109/4.792620

15. RamRakhyani, A. K., Mirabbasi, S., and Chiao, M. (2010) Design and optimization of resonance-based efficient wireless power delivery systems for biomedical implants, *IEEE transactions on biomedical circuits and systems*, 5(1), 48-63. doi: 10.1109/TBCAS.2010.2072782
16. Sahai, A. and Graham, D. (2001) Optical wireless power transmission at long wavelengths, *IEEE International Conference on Space Optical Systems and Applications (ICSOS)*, Santa Monica, 164-170. doi: 10.1109/ICSOS.2011.5783662
17. Sample, A. P., Meyer, D. T., and Smith, J. R. (2010) Analysis, experimental results, and range adaptation of magnetically coupled resonators for wireless power transfer, *IEEE Transactions on industrial electronics*, 58(2), 544-554. doi: 10.1109/TIE.2010.2046002
18. Shuvo, M. M. H., Titirsha, T., Amin, N., and Islam, S. K. (2022) Energy harvesting in implantable and wearable medical devices for enduring precision healthcare. *Energies*, 15(20), 7495. doi: 10.3390/en15207495
19. Tesla, N. (1905) Art of Transmitting Electrical Energy through Natural Mediums, U.S. Patent No. 787,412.

